SCI. MAR., 69 (3): 323-341 SCIENTIA MARINA 2005

Microplankton composition, production and upwelling dynamics in Sagres (SW Portugal) during the summer of 2001*

SOFIA LOUREIRO [1], ALICE NEWTON [2] and JOHN D. ICELY [3]

[1] CMQA-FCT, Gambelas Campus, Univ. Algarve, 8000-117 Faro, Portugal. E-mail: sofia7sky@yahoo.com
[2] IMAR-FCT, Gambelas Campus, Univ. Algarve, 8000-117 Faro, Portugal.
[3] Sagremarisco Lda, Apt 21, 8650 Vila do Bispo, Portugal.

SUMMARY: Microplankton community, production, and respiration were studied alongside physical and chemical conditions at Sagres (SW Portugal) during the upwelling season, from May to September 2001. The sampling station was 5 km east of the upwelling centre off Cabo S. Vicente, and 2 km west of an offshore installation for bivalve aquaculture. Three major periods were distinguished according to sea surface temperature (SST): period 1 (P1; May and June), characterised by high temperature values (17.0±1.8ºC); period 2 (P2; July), characterised by lower temperatures (14.6±0.3ºC), identified as an upwelling-blooming stage; and period 3 (P3; August), characterised by a high temperature pattern (16.25±1.14ºC). *Chaetoceros* spp., *Thalassiosira* spp., *Lauderia* spp., *Detonula* spp. and *Pseudo-nitzschia* spp. were the major taxa contributing to the dissimilarities between P2 (July) and the other periods. In July (P2), the average gross production (GP; 52.5±12.3 μM O_2 d^{-1}) and net community production (NCP; 46.9±15.3 μM O_2 d^{-1}) peaked with the maximal concentrations of diatom-chl *a*. Dark community respiration (DCR) remained low and more constant throughout (4.6±3.6 μM O_2 d^{-1}). The plankton assemblage was dominated by diatoms throughout the survey. Physical events were the primary factors determining the microplankton structure and distribution at this location.

Keywords: production, respiration, microplankton community, Iberian Peninsula, Cabo S. Vicente.

RESUMEN: COMPOSICIÓN DEL MICROPLANCTON, PRODUCCIÓN Y DINÁMICA DEL AFLORAMIENTO EN SAGRES (SUROESTE DE PORTUGAL) DURANTE EL VERANO DE 2001. – La comunidad microplanctónica, la producción y la respiración, fueron estudiadas en Sagres (SE Portugal) durante la época de afloramiento, de Mayo a Septiembre 2001, junto con parámetros físicos y químicos. La estación de muestreo está a 5 km Este del centro de afloramiento del Cabo S. Vicente, y a 2 km Oeste de una instalación para el cultivo de bivalvos. Según los patrones de la temperatura del agua de superficie (SST) se diferenciaron tres periodos: periodo 1 (P1; Mayo y Junio), caracterizado por temperaturas altas (17.0±1.8ºC); periodo 2 (P2; Julio), caracterizado por temperaturas más bajas (14.6±0.3ºC), identificado como un estado de -afloramiento; periodo 3 (P3; Agosto), caracterizado por un patrón de temperaturas altas (16.25±1.14ºC). *Chaetoceros* spp., *Thalassiosira* spp., *Lauderia* spp., *Detonula* spp. y *Pseudo-nitzschia* spp., fueron los principales grupos que contribuyeron a la diferenciación entre P2 (Julio) y el resto de periodos. Durante Julio (P2) la media de producción primaria bruta (GP; 52.5±12.3 μM O_2 d^{-1}) y de producción primaria neta (NCP; 46.9±15.3 μM O_2 d^{-1}) alcanzaron sus valores máximos, simultáneamente con el pico de diatomeas-chl *a*. La respiración de la comunidad en la oscuridad (DCR) permaneció baja y constante durante el muestreo (4.6±3.6 μM O_2 d^{-1}). La comunidad estaba dominada por diatomeas durante todo el muestreo. Los eventos físicos fueron el factor principal en la determinación de la estructura de la comunidad microplanctónica en esta localidad.

Palabras clave: producción, respiración, comunidad microplanctónica, península Ibérica, cabo San Vicente.

*Received May 21, 2004. Accepted January 14, 2005.

INTRODUCTION

Coastal fertilisation by cold nutrient-rich upwelled waters stimulates productivity and phytoplankton blooms (Barber and Smith, 1981). These blooms are dominated initially by non-motile diatoms (Officer and Ryther, 1980) that are preferentially selected under the turbulent conditions produced by strong winds, which are responsible for the upwelling. As the turbulence is reduced, optimal conditions develop for the more motile dinoflagellates, establishing the plankton succession pattern (Margalef, 1978; Smayda, 2000). The ocean biota is sustained by the balance between the autotrophic (i.e. production) and heterotrophic (i.e. respiration) processes (e.g. Williams, 1984, 1998). In coastal systems where inputs from terrestrial sources are limited, such as the studied location, phytoplankton primary production represents the main source of organic matter. Size fractionation studies (Williams, 1981) have associated the dominant respiratory activity in coastal waters with small non-photosynthetic organisms, such as heterotrophic bacteria and microflagellates.

Northerly winds along the west coast of the Iberian Peninsula produce conditions for seasonal upwelling from early spring to late summer (e.g. Wooster *et al*., 1976; Fiúza *et al*., 1982), whilst occasional upwelling occurs along the southern coast of Portugal (Algarve) with favourable westerly winds. After a prolonged period of northerly winds, fertile water can circulate around the Cabo S. Vincente, the southwestern tip of the peninsula, and flow eastwards along the southern coastal shelf (Fiúza, 1983; Sousa and Bricaud, 1992; Relvas and Barton, 2002). In contrast, a warm counter current, originating in the Gulf of Cadiz (Fig. 1) flows westwards to the Algarve coast and, during periods of prolonged southeasterly winds, can circulate around Cabo S. Vincente and flow northwards (Relvas and Barton, 2002). In relation to the overall patterns of ocean circulation in the eastern Atlantic, the northern part of the west coast of the Iberian Peninsula is influenced by the subpolar branch of the Eastern North Atlantic Central Water (ENACWsp), whereas the southern upwelled waters have characteristics of the ENACW subtropical branch (Fiuza, 1984; Ríos *et al*., 1992).

The variations in phytoplankton abundance and composition between the northern and southern part of the west coast are primarily a consequence of the distinct topography of the continental shelves and river runoff (Peliz and Fiúza, 1999). In winter, the freshwater runoff induces salinity stratification on the wider and shallower shelf of the northwest coast, favouring the development of phytoplankton blooms. The peak for seasonal phytoplankton abundance occurs in spring and summer. The summer upwelling community is composed of chain-forming diatoms such as *Pseudo-nitzschia* spp. and *Chaetoceros* spp. (Moita, 2001).

These upwelling systems have supported an important fishery resource for the west coast of the Iberian peninsular. In the case of the Algarve, 12.1% of the total licensed fleet is located at Sagres (Martins and Carneiro, 1997; Pita *et al*., 2002). Furthermore, in recent years, a significant contribution to the local economy has come from the production of 300 tons of oysters at Sagres (Cachola, 1995; European Commission, 1999; pers. comm. Tessier). This aquaculture is dependent on the enrichment of the coastal waters by upwelling as there are no permanent rivers or streams in the area and the anthropogenic contribution is minimal because of the low resident population and limited agriculture.

Despite the importance of the Sagres region for Portuguese fisheries and bivalve culture, studies of production and associated phytoplankton community are scarce. Villa *et al*. (1997) reported a peak in May and September for phytoplankton based on estimates of chlorophyll *a* (chl *a*), and maxima for zooplankton between July and September based on plankton tows. Moita *et al*., (1998) have observed episodic blooms of toxic dinoflagellates east of Cabo S. Vicente along the Algarve coast. Sampayo *et al*. (1997) have detected biotoxins, leading to the temporary closure of oyster sales from Sagres.

This study was undertaken during the upwelling season, from May to September 2001, at Sagres, in order to understand the influence of the circulation and upwelling events on the local microplanktonic population and primary production. The monitoring includes several of the elements required by the European Water Framework Directive (WFD, 2000) to assess the ecological status of coastal waters including physico-chemical parameters (temperature, salinity, oxygen and transparency data) and biological parameters (composition, abundance and biomass of the phytoplanktonic community).

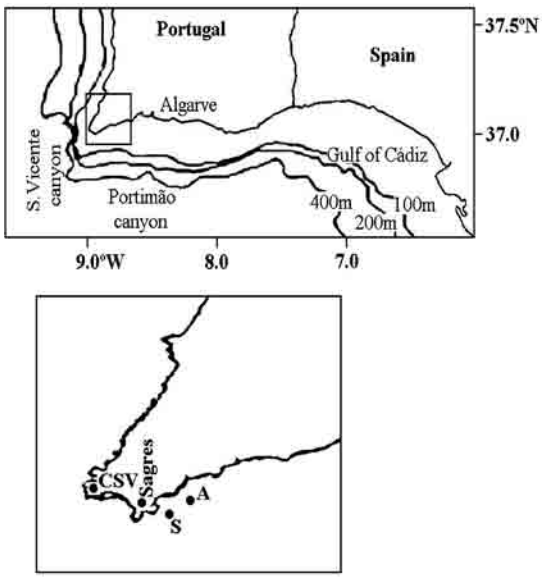

FIG. 1. – Location of the sampling station (S). Cabo S. Vicente (CSV), oyster aquaculture (A).

MATERIAL AND METHODS

Study area

The Algarve coast along southern Portugal extends between 7°20'W and 9°W, along 37°N indented by two major canyons: S. Vicente and Portimão. The west coast off Algarve has an even narrow shelf, about 10 km wide. The sampling station (Fig. 1) was 5 km east of the upwelling centre off Cabo S. Vicente, at the entrance to the Porto Baleeira at Sagres (37°00'63" N and 8°55'62"W), and 3 km west of an offshore "long-line" system for oyster culture (37°00'40"N and 8°53'75"W). Following the requirements of the Water Framework Directive (WFD, 2000), this area is classified as a mesotidal, moderately exposed, coastal water of the Atlantic type (Bettencourt *et al*., 2004). The location was recently selected as an intercalibration site for the Common Implementation Strategy of the WFD.

Sampling

The Sagres station was sampled weekly, between the end of May and the beginning of September, with an interruption of 19 days in June. Surface water was collected early in the morning, independently of the tidal phase, and filtered through a 200μm mesh size net, to select for the microplankton community and remove the larger grazing organisms and particles. Aliquots for nutrients determination were frozen at -20 ºC for later analysis of ammonium, nitrite, nitrate, phosphate, and silicate, according to the methods described in Grasshoff *et al*. (1983). Chl *a* concentration was determined by further filtering 1 l of water sample, through a Whatman GF/F filter, for measurement with a Jasco FP-777 based on the fluorometric methods described by JGOFS (1994).

Water transparency was determined by Secchi-disc depth and used for the estimation of the percentage irradiation depth profile. In general, the euphotic zone (defined as the depth at which the light intensity is 1% of the intensity of the surface) was greater than the overall depth of the sample site, which averaged 20 ± 3m depending on tidal fluctuations. Water for the determination of the dissolved oxygen concentration was collected with a Niskin bottle from depths at which the light intensity was 100, 50, 25 and 10% of that at the surface. Oxygen concentrations were determined with triplicates of each sample by the Winkler method (Strickland and Parsons, 1972; Bryan *et al*., 1976) using a Brand microburette for the titrations and expressing the final concentrations as μM O_2 (± SE).

Sea surface temperature (SST) was recorded with a Tinytalk PT 100 logger attached to a "long-line" for oyster culture. Total daily solar irradiance (KJ m^{-2}) was recorded by the Portuguese Instituto de Meteorologia (IM) at the Sagres station (8°57'W, 37°00'N, 25 m). Irradiance was converted to photosynthetically available radiation (PAR) using the criteria that PAR roughly represents 45% of total solar radiation (Kirk, 1994). PAR values for the surface layer were estimated based on the equation:

$$I_z = I_0 e^{-k z} \quad (1)$$

where I_0 is the incident radiation, I_z the radiation at z depth, and k the Secchi extinction coefficient (Kirk, 1994).

Apart from the 24 July, temperature and salinity profiles were recorded with a Seacat SBE 19 CTD between July and the end of the survey in September. The density (σ_t) was calculated from temperature and salinity data according to the algorithms of Fofonoff and Millard (1983).

Upwelling indices

The Ekman transport of surface water was estimated according to Bakun's (1973) method, and used as a coastal upwelling index:

$$q_{x,y} = \frac{\tau_{x,y}}{f\rho_w} = \frac{\rho_a C_D |V| V_{x,y}}{f\rho_w} \quad (2)$$

where $\tau_{x,y}$ is the wind stress vector, ρ_a is the air density (1.22 Kg m^{-3}), C_D is an empirical dimensionless drag coefficient (1.14x10^{-3}, see Large and Pond, 1982), $V_{x,y}$ is the wind speed vector on the sea surface, with magnitude $|V|$, f is the Coriolis parameter (8.78x10^{-5} s^{-1} for Sagres), and ρ_w is the density of seawater (~1025 Kg m^{-3}).

Wind direction and magnitude were obtained from the IM station at Sagres. The wind stress vector was divided into its two components (τ_x the eastward component, and τ_y the northward component), giving an estimation of q_x and q_y (m^3 s^{-1} km^{-1}) for Ekman transport. Positive values for q_x indicate upwelling-favourable offshore Ekman transport along the south coast, whereas negative values of q_x represent inshore Ekman transport on the south coast. Conversely, positive values of q_y indicate downwelling on the west coast, whilst negative values of q_y indicate upwelling-favourable offshore Ekman transport along the west coast.

Production and respiration rates

Production and respiration rates were estimated by the oxygen light-dark bottle technique (Strickland and Parsons, 1972). The filtered samples were siphoned carefully into 300 ml Winkler bottles with silicon tubing to reduce turbulence. Triplicates were fixed immediately for measurement of initial dissolved oxygen concentrations. Triplicates of light and dark bottles were suspended along a 'long-line' and incubated for 24 h, after which they were fixed.

Gross production (GP), net community production (NCP) and dark community respiration (DCR) were determined from the difference between the means of the light, dark, and initial time replicates; rates are expressed as μM O$_2$ d^{-1} (±SE). Rates were converted to carbon units using 1.4 as the photosynthetic quotient (Laws, 1991).

Microplankton identification and carbon content

Microplankton samples were preserved with acidified Lugol's iodine solution. Each sample was placed in a 100 ml sedimentation chamber and settled for observation with a Zeiss Axiovert 25 inverted microscope. Qualitative and quantitative analyses of the samples were based on the methods of Utermöhl (1958). Smaller cells were identified (Tomas, 1997) and counted at 400x magnification up to a total of 100 optical fields, whereas the less abundant and larger organisms were observed over

TABLE 1. – Surface values of physical, biological, and chemical parameters (± SD); *n*, number of observations: min, minimum value; max, maximum value; PAR, photosynthetically available radiation; Sal., salinity; σ_t, density; photic = euphotic layer; T, temperature; NCP, net community production; GP, gross production; DCR, dark community respiration; chl *a*, chlorophyll *a* concentration; NH_4^+, ammonium concentration; NO_2, nitrite concentration; NO_3, nitrate concentration; SiO_4, silicate concentration; O_2, oxygen concentration.

Period	PAR 10^3KJm^{-2}d^{-1}	Sal.	σ_t Kg m^{-3}	Secchi m	Photic m	T °C	NCP μM O$_2$ d^{-1}	GP μM O$_2$ d^{-1}	DCR μM O$_2$ d^{-1}	Chl *a* μg l^{-1}	NH_4^+ μM	NO_2^- μM	NO_3^- μM	PO_4^{3-} μM	SiO_4^- μM	O_2 μM
P1	12.6±4.2	35.9±0.0	26.1±0.2	10±3	26±9	17.0±1.8	12.5±7.5	16.2±8.7	3.7±2.0	1.8±0.5	0.6±0.6	0.2±0.1	8.4±3.1	0.3±0.1	1.1±0.7	237±9
	(***n***=5)	(*n*=2)	(*n*=2)													
min	11.9	35.9	26.0	7	19	14.7	5.1	8.3	2.2	1.2	u.d.l.*	0.1	4.3	0.2	0.4	227
max	12.9	35.9	26.3	14	40	19.2	20.9	28.1	7.2	2.4	1.5	0.3	11.6	0.4	1.9	247
P2	11.1±1.5	35.8±0.1	26.6±0.2	8±1	21±3	14.6±0.3	47.5±14.5	53.0±9.9	5.5±5.2	5.6±0.6	0.3±0.2	0.2±0.1	12.7±5.9	0.3±0.1	0.6±0.4	258±15
	(*n*=4)	(*n*=3)	(*n*=3)													
min	8.9	35.7	26.4	7	19	14.3	26.3	39.6	1.8	4.8	0.1	0.1	6.2	0.2	0.1	246
max	12.2	35.8	26.7	9	24	14.9	57.1	60.6	13.3	6.2	0.5	0.2	19.3	0.4	1.0	279
P3	10.1±1.3	35.8±0.1	26.2±0.3	8±2	22±5	16.2±1.1	8.5±8.0	12.6±7.7	4.1±2.0	3.1±0.9	0.3±0.1	0.3±0.1	10.2±3.8	0.3±0.1	1.2±0.9	241±10
	(*n*=5)	(*n*=5)	(*n*=5)													
min	8.0	35.7	25.8	7	19	14.8	-3.9	2.4	1.0	1.7	0.2	0.1	5.9	0.2	0.3	225
max	11.1	35.8	26.5	11	30	17.5	16.4	19.9	6.3	4.0	0.4	0.4	16.0	0.4	2.4	8.9
Total	11.3±15.3	35.8±0.1	26.6±0.4	9±2	23±6	16.0±1.6	21.1±19.7	25.4±19.8	4.3±3.1	3.3±1.7	0.4±0.4	0.2±0.1	10.3±4.3	0.3±0.1	1.0±1.7	244±13
	(*n*=14)	(*n*=10)	(*n*=10)													
min	8.0	35.7	25.8	7	19	14.8	-3.9	2.4	1.0	1.2	u.d.l.*	0.1	4.3	0.2	0.1	225
max	12.9	35.9	26.6	14	40	19.2	57.1	60.6	13.2	6.2	1.52	0.4	19.3	0.4	2.4	279

u.d.l.* denotes under detection limits

the entire chamber at 100x magnification. Organisms were generally identified down to genus and whenever possible to species level; whenever this classification was not possible cells were included in wider groups (see Table 3). Cell volumes were determined by approximation to the nearest geometric shape (Hillebrand *et al*., 1999), and converted to biomass carbon units on the basis of formulae devised by Verity and Langdon (1984) and Verity (1992).

Analysis of microplankton assemblage

A statistical study of the microplankton community was completed with PRIMER© software (Plymouth Routines In Multivariate Ecological Research) for a multivariate analysis of the microplankton community. An assessment of natural groupings within the community was completed by multi-dimensional scaling (MDS) ordination using the Bray-Curtis similarity matrices of square-root abundance and biomass data. Significance tests for differences between the *a priori* established groups were carried out using one-way analysis of similarities (ANOSIM in Clarke and Warwick, 2001). The contribution of taxa to dissimilarities between the different periods (see results for period's definition) were evaluated using the routine for similarity percentages (SIMPER in Clarke, 1993). The non-parametric statistical tests were done with the STATISTICA© 6 program.

RESULTS

Stages of the upwelling season

Three periods were distinguished on the basis of the changes in SST during the survey (Table 1): period 1 (P1), from 24 May to 10 July, corresponded to a high temperature stage prior to a persistent upwelling event; period 2 (P2), from 11 July to 31 July, was marked by lower temperatures corresponding to a major upwelling event; finally, period 3 (P3), from 1 August to 3 September, corresponded to a further stage of higher temperatures.

Wind and hydrographic conditions

Figure 2 summarises both the speed distribution and the direction of the wind, and Figure 3b is a stick vector diagram of the time-series for coastal wind

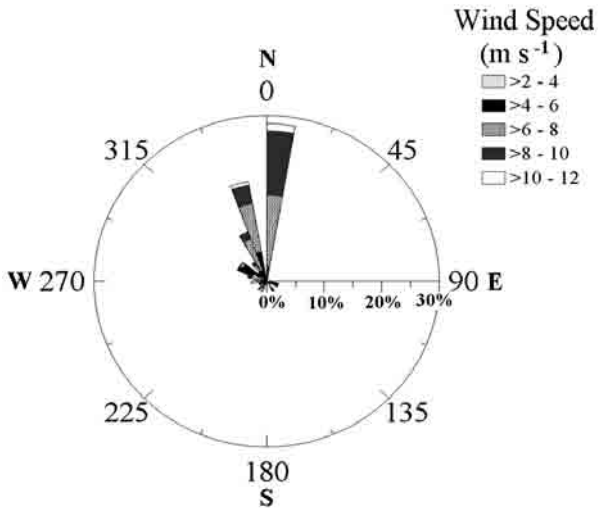

FIG. 2. – Chart of wind direction and speed distribution (%) from May to September 2001 at Sagres.

speeds. Both figures show the prevailing northerly wind regime, from May to September, with average velocities of 6-10 m s^{-1}. At the beginning of May (P1), favourable conditions for upwelling on the south coast (inferred by q_x >0, Fig. 3a) induced a period of low SST (14ºC), followed by conditions favourable for upwelling on the west coast (inferred by q_y < 0). The increasing SST by the end of May was related to a brief reversal in wind direction, leading to the replacement of cold water by warmer waters from the intrusion of the counter current from Cadiz towards the study site at Sagres. In June (P1), the generally high wind velocities and the persistent upwelling on the west coast (q_y decreased to -700 m^3 s^{-1} km^{-1}) were linked to a decline in local SST (min. 15ºC), suggesting the influence of western, upwelled cold waters on the Sagres site. An increase in SST was recorded in the last week of June (max. 18°C), probably reflecting the relaxation of the upwelling conditions on the south coast (q_x < 0) followed by the intrusion of the warmer coastal counterflow (07 and 25 June in Fig. 4). During the first few days of July (P2) an upwelling plume extended eastward from Cabo S. Vicente (03 June in Fig. 4) but had still not arrived at Sagres sampling station. In July (P2), SST reached the minimal values, associated with q_x and q_y favourable to offshore transport. On 11 July cold waters were mainly located south of the Cabo S. Vicente region, with a slight eastward advection extending up to Sagres (Fig. 4). During the rest of the month cold waters extended along the shelf off the Algarve. In August (P3), the SST at Sagres (Fig. 3d) reflected the variability of the wind regime with a cycle of upwelling / relaxation events with a duration

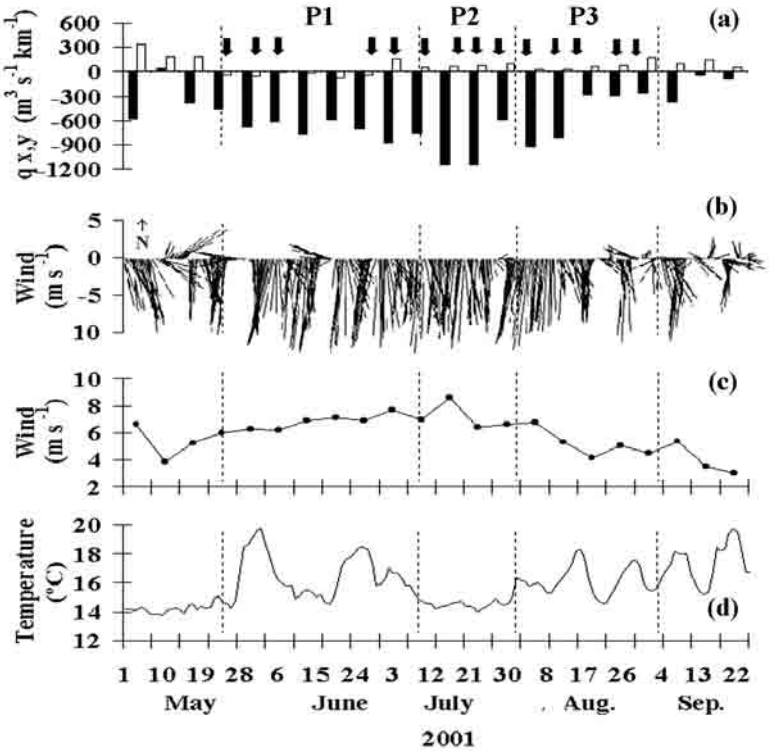

FIG. 3. – Temporal evolution of (a) mean weekly eastward (q_x , white bar) and northward (q_y, black bar) Ekman transport ($m^3 s^{-1} km^{-1}$); positive q_x values indicates upwelling favourable conditions for the south coast, whereas negative q_y represents upwelling favourable conditions for the west coast; (b) wind vectors time series between May and September 2001; (c) mean weekly wind speed, and (d) sea surface temperature (SST; ºC) at the sampling location. Arrows indicate sampling dates. Periods 1, 2 and 3 (P1, P2 and P3 respectively) mark stages of the upwelling season, defined according to the temperature ranges (see results).

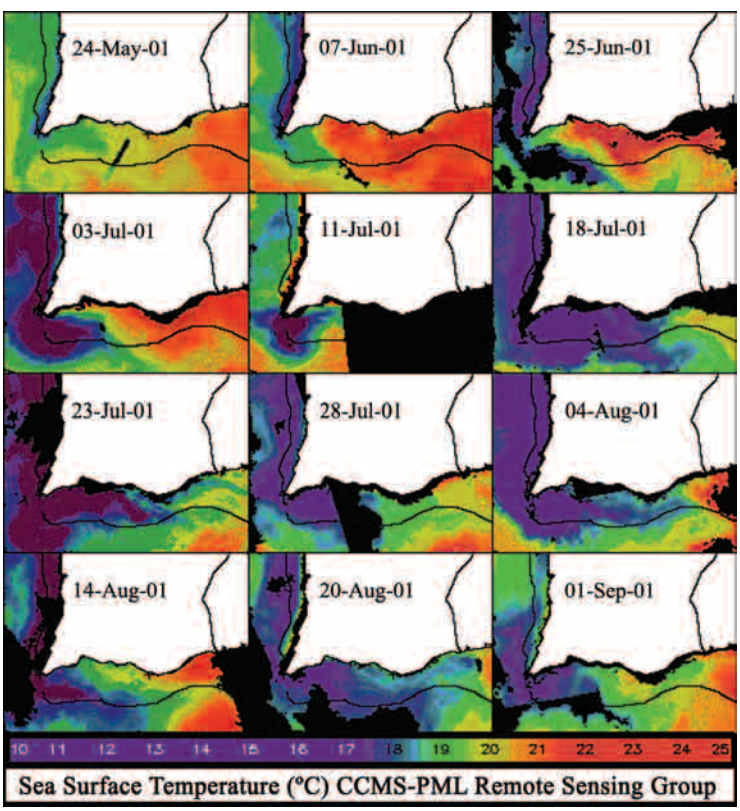

FIG. 4. – Sea Surface Temperature (SST) satellite images (NOAA/AVHRR) from the South of Portugal (Algarve), processed at the Plymouth Marine Lab, UK. Dates are indicated in the images.

TABLE 2. – Spearman rank-order correlation between biological, chemical and physical parameters determined during the sampling season: net community production (NCP, μM O_2 d^{-1}), gross production (GP, μM O_2 d^{-1}), dark community respiration (DCR, μM O_2 d^{-1}), chlorophyll *a* concentration (Chl *a*, μg l^{-1}), temperature (T, ºC), nitrate (NO_3, μM), diatom ([diat]), dinoflagellate ([dino]), nanoflagellate ([nano]), ciliate ([cilia]) and total microplankton abundance ([total], x10^3 cell. l^{-1}) and biomass (BMdiat, BMdino, BMnano, BMcilia, Bmtotal, μgC l^{-1}), oxygen concentration ([O_2], μM), eastward (q_x) and northward (q_y, m^3 s^{-1} km^{-1}) Ekman transport component. Bold figures are significant at $p < 0.05$; *n* represents the number of samples.

n = 14	NCP	GP	DCR	Chl *a*	T	NO_3	[diat]	[dino]	[nano]	[cilia]	[Total]	BMdiat	BMdino	BMnano	BMcilia	BMtotal	[O_2]	q_x	q_y
NCP	1																		
GP	**0.99**	1																	
DCR	0.03	0.08	1																
Chl *a*	**0.78**	**0.77**	0.15	1															
T	**-0.74**	**-0.70**	0.45	**-0.70**	1														
NO_3	0.32	0.25	**-0.56**	0.30	**-0.63**	1													
[diat]	**0.78**	**0.82**	0.33	**0.87**	**-0.60**	0.18	1												
[dino]	-0.44	-0.48	0.50	-0.20	**0.65**	-0.36	-0.30	1											
[nano]	-0.52	**-0.54**	-0.06	-0.41	0.31	0.11	-0.32	0.35	1										
[cilia]	-0.31	-0.24	**0.62**	-0.31	**0.64**	**-0.71**	-0.17	0.49	-0.20	1									
[Total]	**0.76**	**0.78**	0.45	**0.89**	-0.47	0.01	**0.96**	-0.05	-0.30	0.04	1								
BMdiat	0.44	0.44	0.20	**0.79**	**-0.55**	0.32	**0.75**	-0.21	-0.16	-0.27	**0.67**	1							
BMdino	-0.19	-0.25	0.27	-0.18	0.42	-0.38	-0.37	**0.65**	-0.14	0.38	-0.20	-0.24	1						
BMnano	-0.33	-0.38	0.03	-0.24	0.30	0.11	-0.24	0.49	**0.66**	-0.27	-0.17	-0.13	0.24	1					
BMcilia	-0.26	-0.23	0.25	-0.37	0.38	-0.47	-0.27	0.30	-0.02	**0.72**	-0.24	-0.15	0.43	-0.13	1				
BMtotal	0.43	0.41	0.21	**0.78**	-0.45	0.11	**0.63**	-0.12	-0.34	-0.19	0.59	**0.91**	0.06	-0.18	-0.08	1			
[O_2]	**0.66**	**0.65**	0.22	**0.78**	-0.51	-0.13	**0.66**	-0.13	-0.50	-0.06	**0.71**	**0.54**	0.08	-0.17	-0.09	**0.66**	1		
q_x	0.47	0.42	-0.22	0.53	**-0.67**	0.19	0.31	-0.22	-0.40	-0.30	0.30	0.31	0.07	-0.36	-0.12	0.40	0.43	1	
q_y	-0.48	-0.45	-0.00	-0.52	**0.56**	-0.42	**-0.57**	0.45	0.10	0.38	-0.41	**-0.75**	0.28	0.01	0.16	0.16	-0.45	0.01	1

of 14 days. Along the south continental shelf, episodes of relaxation were associated with the influence of the warm counter current. The selected SST satellite images (Fig. 4) are representative of P1 (24 May-3 July), P2 (11 July-28 August) and P3 (4 August-1 September).

Local SST was negatively correlated (Spearman; $p<0.05$) with average weekly values for q_x taken from the previous 7 days, and positively correlated with average weekly values for q_y (Table 2) over the period of the survey. Overall, the upwelling events adjacent to Sagres seemed to be influenced by the interplay between water circulation driven by the winds along the west and south coasts.

Time-series of depth profiles

Figure 5 shows a series of depth profiles for O_2 and temperature measured during the survey.

24 May - 10 July (P1). At the beginning of the study the water column was homogeneously oxygenated (248±0.3 μM O_2, n = 12). On 31 May, the SST maximum was complemented by a minimal oxygen concentration at the surface (233±0.2 μM O_2). In June, the two available oxygen profiles presented similar distribution patterns, and by 3 July a subsurface (9.5 m) minimal oxygen value (222±0.2 μM O_2) indicated the possibility of intrusion at Sagres of oxygen-deficient, upwelled waters.

11 July - 31 July (P2). This period of mature-upwelling was characterised by colder temperatures at all depths. On 11 July, the thermocline (0.2°C m^{-1}) was at a depth of 11 m. By 18 July, the surface water was warmer, and a steeper (0.4°C m^{-1}), shallower (6 m) thermocline had developed: salinity and density (σ_t) profiles (Fig. 6) demonstrated a stratification on this date. However, oxygen profiles were generally homogeneous. On 31 July, high pelagic oxygen concentrations (277±2 μM O_2, n = 12) probably reflected a recent active blooming phase. The pycnocline was associated with a less saline surface layer.

1 August - 3 September (P3). The oxygen decreased, as is typical of post-blooming periods. On 14 August there was an increase in surface stratification (pycnocline of 5-10 m) associated with a warmer, less saline layer. This probably reflects the intrusion of the warm coastal countercurrent coming from the Gulf of Cádiz. On 20 August there was a steep shallow thermocline (4 m), below which was a layer of both low oxygen (227±1 μM O_2, n = 6) and low temperature (13.8ºC). The subsurface oxygen

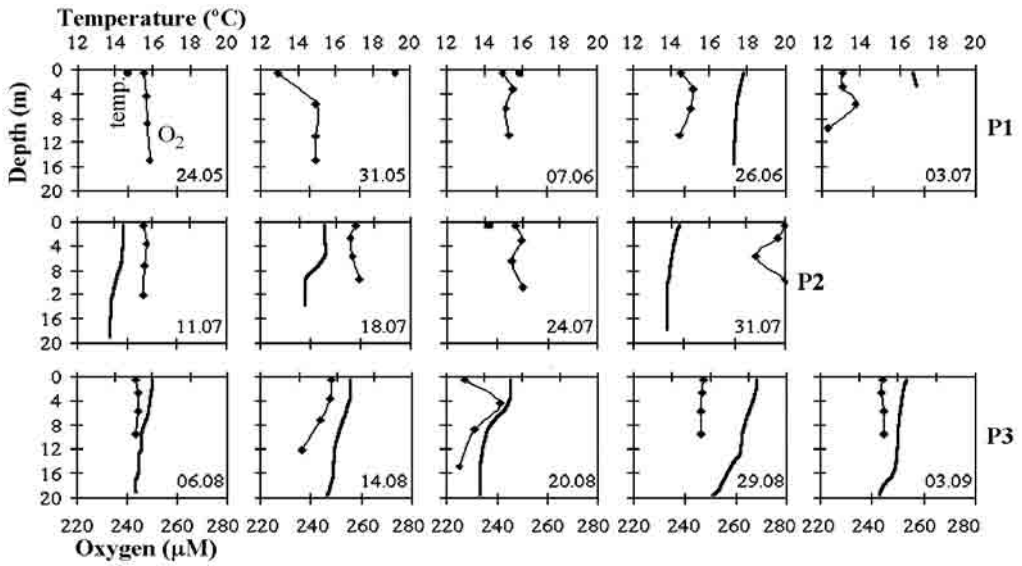

FIG. 5. – Vertical profiles of oxygen concentrations (μM O_2), and temperature (ºC) taken from available CTD casts; when CTD casts were not available, temperature data are from a logger (see Material and Methods). Sampling date is shown on each plot. P1, P2 and P3 denote the three distinct upwelling periods.

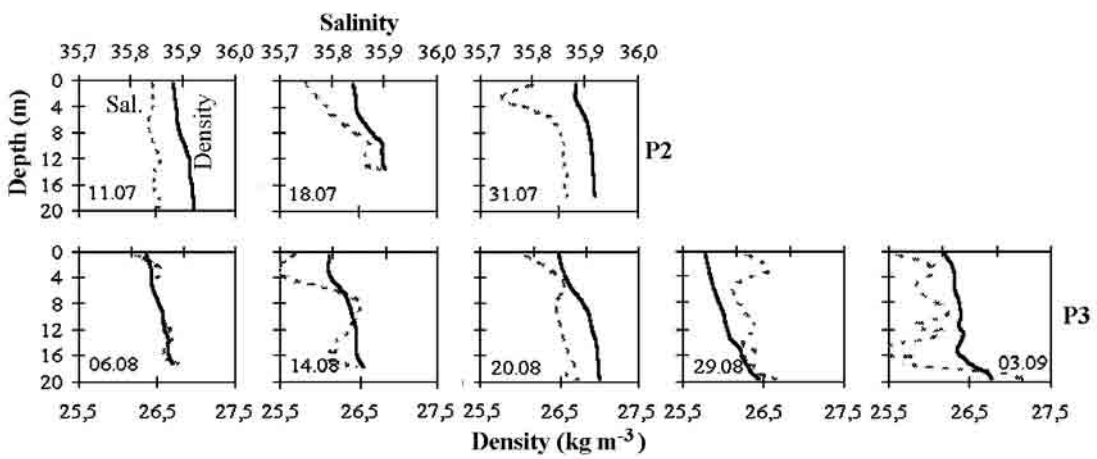

FIG. 6. – Vertical profiles of salinity (dashed line), and density (dark line) taken from available CTD casts. Sampling date is shown on each plot. P2 and P3 denote the distinct upwelling periods.

maximum (241±0.2 μM O_2) was at 3 m adjacent to the thermic surface layer. The water column temperature rose towards the end of August (max. 18°C), but declined rapidly in September (min. 16°C), reflecting the relaxation / upwelling cycles referred to previously.

Physical, biological and chemical parameters

Table 1 summarises the ranges of surface physical, chemical and biological parameters. PAR was high throughout the survey, with a maxima during P1 (Fig. 7b). The density attained a maximum (26.7 kg m^{-3}) in July (P2), confirming the upwelling of denser water masses. The highest transparency values for the water column (Fig. 7a) were recorded at the beginning of the study and on 20 August (11 m). The depth of the euphotic layer, calculated from Secchi disk data, was 19-40 m in May-June (P1). This was reduced to 19-24 m during the July (P2) upwelling/blooming event and then increased in August (P3) to 19-30 m.

In May-June (P1), chl*a* surface values averaged 1.8±0.5 μg l^{-1}, followed by a significant increase during the July (P2; ANOVA p <0.0001, *post hoc* LSD Fisher test) upwelling episode (Fig. 7a), with the maximum of 6.2 μg l^{-1}. The August (P3) decline (min. 1.7 μg l^{-1}) was followed by a steady rise until the end of the survey, implying the development of a new bloom.

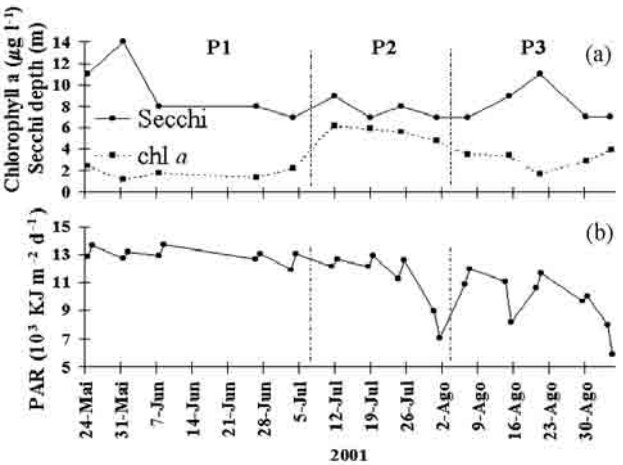

FIG. 7. – Temporal distribution of surface (a) chlorophyll *a* concentration (μg l^{-1}), Secchi depth (m), and (b) photosynthetically available radiation (PAR; 10^3 KJ m^{-2}d^{-1}) from 24 May to 3 September 2001 at the Sagres station.

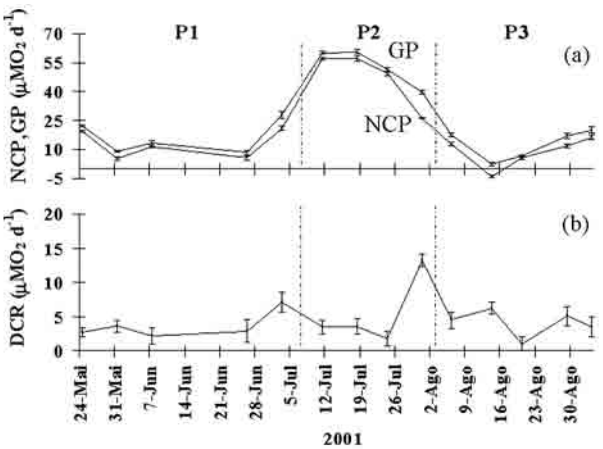

FIG. 8. – Temporal distribution of surface (a) net community production (NCP), gross oxygen production (GP) and (b) dark community respiration (DCR) rates (μM O$_2$ d^{-1}), based on the light-dark bottle method, 24 h incubation, from 24 May to 3 September at the Sagres station. Bars correspond to standard errors; where the bars are not visible the data hid the small errors.

The mean coefficient of variation (CV) for initial, "light", and "dark" oxygen bottles was 0.56% (n = 42), 0.49% (n=42), and 0.72% (n = 42) respectively. The mean of the standard errors for primary production and respiration rates were: 0.84 μM O$_2$ d^{-1} (n=14) for NCP, 1.02 μM O$_2$ d^{-1} (n=14) for GP, and 1.07 μM O$_2$ d^{-1} (n=14) for DCR. The distribution of production rates (Fig. 8a) exhibited a similar pattern to chl *a* (max. GP, 61±1.4 μM O$_2$ d^{-1}; NCP, 57±1.5 μM O$_2$ d^{-1}), although minimal values were observed in August (P3) instead of May-June (P1), both for NCP (-4±0.7 μM O$_2$ d^{-1}) and GP (2±0.8 μM O$_2$ d^{-1}). The NCP minimum corresponded to a period of net heterotrophy (negative NCP) on 14 August. A high significant correlation (Spearman, p< 0.05) between production and chl *a* (Table 2) was observed. DCR remained low throughout the survey (Fig. 8b), reaching its peak (13±1 μMO$_2$ d^{-1}) on 31 July. This date marked the end of a major bloom and was concurrent with a decrease in chl *a* and a minimal value for PAR. Rates in carbon units averaged 180± 169 mg C m^{-3} d^{-1} for NCP, 218± 170 mg C m^{-3} d^{-1} for GP, and 37± 26 mg C m^{-3} d^{-1} for DCR (n=14).

Pulses of nitrate-rich waters (> 12 μM) fertilised the surface from July to August (P2 and P3; Fig. 9a). Each pulse was followed by a decrease in concen-

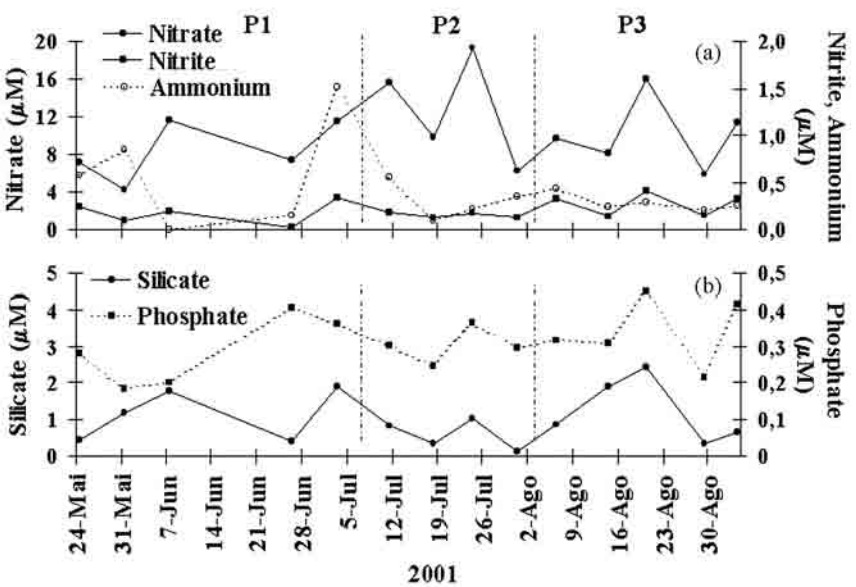

FIG. 9. – Temporal surface distribution of (a) nitrate, ammonium, nitrite, (b) phosphate and silicate concentration (μM) from 24 May to 3 September at the Sagres station.

TABLE 3. – List of identified microplankton taxa, its codes, and frequency of occurrence during the survey. Most frequent taxa (≥50%) in **bold** type.

Code	Taxa	Frequency (%)	Code	Taxa	Frequency (%)
Bacillariophyceae (Diatoms)			**Dinophyceae (Dinoflagellates)**		
Centrales			Ale	*Alexandrium* spp.	14
Ast	*Asteromphalus* spp.	14	Amp	*Amphidinium* spp.	**79**
Bac	*Bacteriastrum* spp.	21	Cer	*Ceratium* spp.	**79**
Cha	*Chaetoceros* spp.	**86**	Dic	*Dicroerisma psilonereiella*	14
Cos	*Coscinodiscus* spp.	36	Din	*Dinophysis* spp.	**57**
Dac	*Dactyliosolen* spp.	**71**	Gon	*Gonyaulax* spp.	7
Det	*Detonula* spp.	36	Gym	*Gymnodinium* spp.	**86**
Euc	*Eucampia* spp.	**57**	GmGr	*Gymnodinium+Gyrodinium* spp.	**100**
Gui	*Guinardia* spp.	**64**	Gyr	*Gyrodinium* spp.	**86**
GuiF	*Guinardia flaccida*	**57**	Kat	*Katodinium* spp.	36
GuiS	*Guinardia striata*	21	Oxy	*Oxytoxum* spp.	7
Hem	*Hemiaulus* spp.	**50**	ProC	*Prorocentrum* spp.	**57**
Lau	*Lauderia* spp.	**93**	ProP	*Protoperidinium* spp.	**93**
Lep	*Leptocylindrus* spp.	**100**	Scr	*Scrippsiella* spp.	**57**
Lic	*Licmophora* spp.	43	Tor	*Torodinium* spp.	36
Mel	*Melosira* spp.	29	DNs	Small < 20 μm Unidentified	**79**
Odo	*Odontella* spp.	**57**	DNb	Big > 20 μm Unidentified	36
Rhi	*Rhizosolenia* spp.	**100**	**Ciliatae**		
Ske	*Skeletonema* spp.	**57**	Hap	Haptorida	**50**
ThaS	*Thalassiosira* spp.	**64**	Mes	Mesodiniidae	**57**
DCs	Small <20 μm Unidentified	**79**	Oli	Oligotrichida	**100**
DCb	Big >20 μm Unidentified	**79**	Tin	Tintinnina	36
Pennales		Cil	Unidentified		43
AstP	*Asterionellopsis* spp.	21	**Cryptophyceae**		
Dip	*Diploneis bombus*	29	Cry	Cryptomonadales	**86**
Fra	*Fragilariopsis* spp.	29	**Dictyochophyceae**		
Man	*Manguinea* spp.	29	Dic	Dictyochaceae(Sillicoflagelates)	29
Meu	*Meuniera membranacea*	29	Ped	Pedinellaceae	36
Nav	*Navicula* spp.	**71**	**Nanoflagellates**		
Nit	*Nitzschia* spp.	**100**	Nan	Unidentified	**100**
Ple	*Pleurosigma* spp.	21			
PSN	*Pseudo-nitzschia* spp.	**93**			
ThaN	*Thalassionema* spp.	21			
DPb	Big (>20 μm) Unidentified	**71**			

tration, suggesting an autotrophic consumption. There was a significant negative correlation (Spearman, $p < 0.05$) between nitrate and SST (Table 2). Ammonium, silicate, and phosphate (Fig. 9a, b) remained low throughout the study; silicate reached a minimal value (0.1 μM) during the diatom-bloom in July (P2), and ammonium peaked twice in May-June (P1). Surface oxygen concentrations were significantly higher (ANOVA, $p = 0.041$, *post hoc* LSD Fisher test) in July (P2; max. 281±0.2 μM O_2).

Microplankton abundance, biomass and composition

A total of 58 microplankton taxa were identified (Table 3) during the survey. From the analysis of microplankton composition, four groups were distinguished: diatoms, dinoflagellates, ciliates, and nanoflagellates; the latter included Crytophyceae, Dictyochophyceae, and nanoflagellates. Bacillariophyceae were the best represented (32), followed by Dinophyceae (17), Ciliatae (5), Dictyochophyceae (2), Cryptophyceae (1) and nanoflagellates (1). The highest occurrences (> 50%) were recorded for five diatoms *(Lauderia* spp., *Leptocylindrus* spp., *Rhizosolenia* spp., *Nitzschia* spp. and *Pseudo-nitzschia* spp.), two dinoflagellates *(Gymnodinium+Gyrodinium* spp., and *Protoperidinium* spp.), one ciliate (Oligotrichida) and the nanoflagellate group.

The temporal evolution of diatom abundance (Fig. 10a) showed a similar trend to those reported for chl *a* and production rates, reflecting the high significant ($p < 0.05$) correlation between these variables (Table 2). Maximum diatom abundance was recorded in July (P2; range: 936-1366 $x10^3$ cell. l^{-1}), and at the end of August (P3). Highest abundances for dinoflagellates were observed on 26 June (110 $x10^3$ cell. l^{-1}) and at the end of the sampling season (> 130 $x10^3$ cell. l^{-1}). Diatom abundance was significantly higher in July (P2; ANOVA $p = 0.002$, *post hoc* LSD Fisher), whereas dinoflagellate abundance was significantly higher in August (P3; ANOVA $p = 0.02$, *post hoc* LSD Fisher). Ciliate abundances

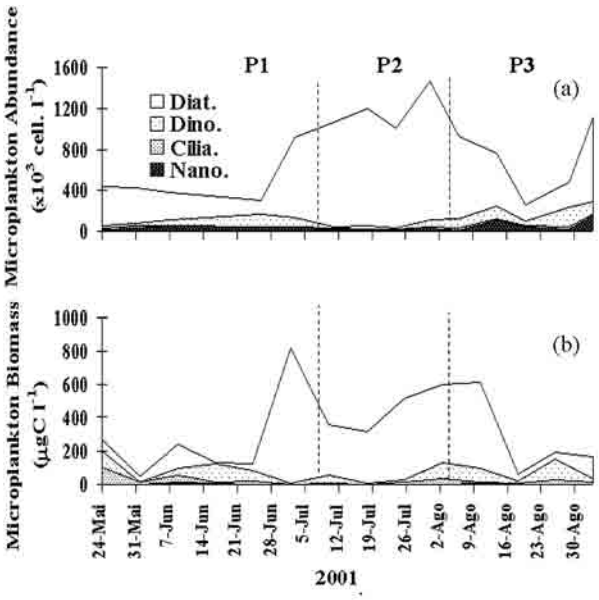

FIG. 10. – Temporal distribution of (a) abundance (10^3 cell. l^{-1}) and (b) biomass (μgC l^{-1}), from the identified functional groups (diat = diatoms, dino = dinoflagellates, nano = nanoflagellates, cilia = ciliates) from 24 May to 3 September 2001 at the Sagres station.

remained low (< 30 x10^3 cell. l^{-1}) throughout the study, whereas nanoflagellates peaked (> 100 x10^3 cell. l^{-1}) during P3, on 14 August and 3 September.

Temporal variations in biomass are shown in Figure 10b: diatom biomass reached mean values of 62±53 (n = 5), 479±238 (n =4) and 240±236 (n = 5) μgC l^{-1} for May-June (P1), July (P2) and August (P3) respectively. Dinoflagellate biomass reached higher values in May-June (P1) and August (P3). The contribution of nanoflagellates to the biomass was low throughout the study (maximum < 15 μgC l^{-1}), whilst the biomass of the oligotrichida and tintinnina ciliates was dominant in May-June (P1) and August (P3).

The changes in relative composition of the systematic groups in each period are evaluated in Figure 11a, b. There was a clear dominance of diatom abundance throughout the survey, reaching a peak (95%) in July (P2). May-June (P1) showed a biomass with a balanced composition of diatoms (37%), dinoflagellates (38%) and ciliates (22%). The biomass contribution of dinoflagellates in May-June (P1) was mainly due to *Protoperidinium* spp. and *Ceratium* spp. Tintinnina and oligotrichida were confirmed as the principle contributors to the biomass of ciliates.

Statistical assemblage analysis

The MDS plots evidenced three distinct groupings corresponding to the May-June (P1), July (P2), and August (P3) stages, both for abundance (Fig. 12

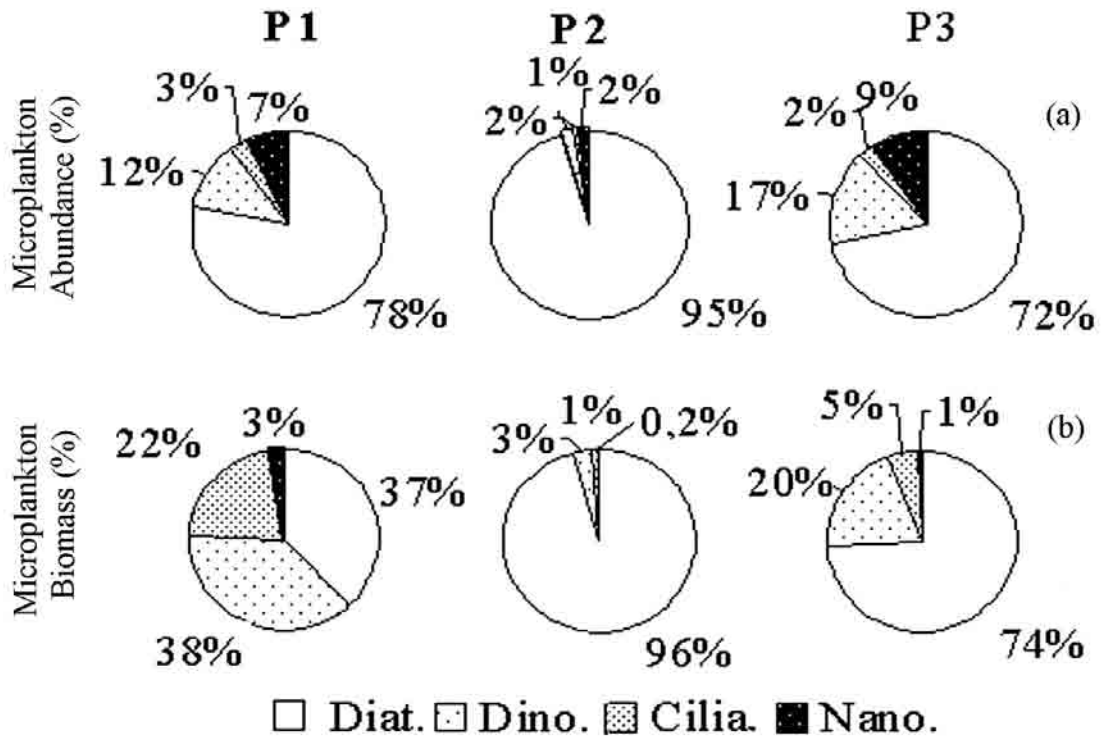

FIG. 11. – Relative (a) abundance and (b) biomass of the microplankton groups in each period (P1, P2 and P3). Each segment represents the total percentage of the respective group (diat = diatoms, dino = dinoflagellates, nano = nanoflagellates, cilia = ciliates).

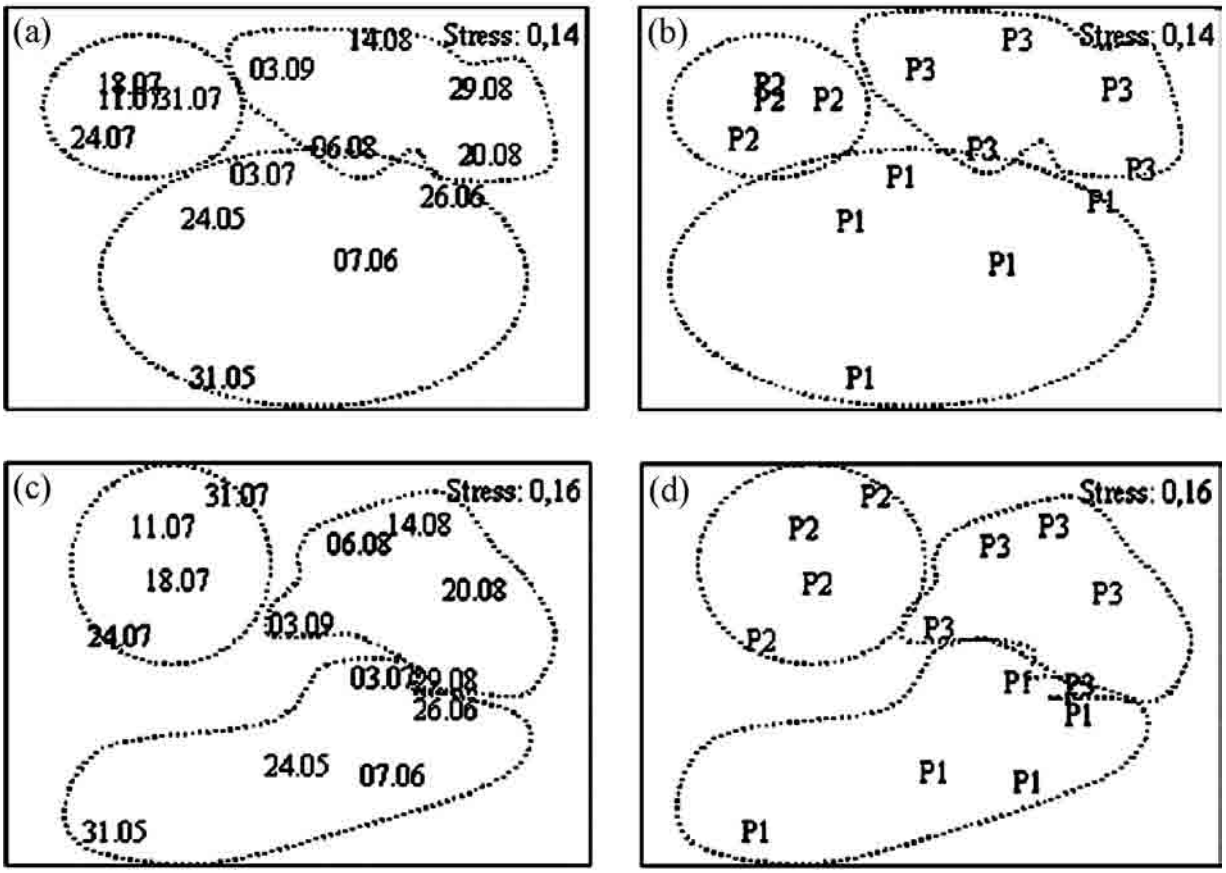

FIG. 12. – Two dimension MDS ordination of Bray-Curtis similarities, from square root transformed abundance (a), (b) and biomass (c), (d). Numbers correspond to sampling dates (day.month). P1, P2, and P3 (the defined sampling periods) groupings are delimited on each plot.

a, b) and for biomass (Fig. 12 c, d). The global R (a statistical measure of the degree of separation of groups) resulting from the one-way ANOSIM tests for abundance data (Table 4) implied the rejection of the null hypothesis (no assemblage differences between P1, P2 and P3) at the 0.002 significance level. However, the pairwise R values (resulting from the comparison of the specific pairs of groups)

TABLE 4. – One-way ANOSIM test for microplankton assemblage differences (in square root transformed abundance and biomass data) between the three *a priori* groups (P1, P2 and P3).

Periods	R pairwise test	Possible permutations	Significance level
(a) Abundance			
Global R = 0.574		999	0.002
P1-P2	0.563	126	0.024
P1-P3	0.368	126	0.008
P2-P3	0.825	126	0.008
(b) Biomass			
Global R = 0.589		999	0.001
P1-P2	0.625	126	0.016
P1-P3	0.452	126	0.016
P2-P3	0.756	126	0.008

showed a weak separation (R = 0.37) between the community structures in May-June (P1) and August (P3). The May-June (P1) and July (P2) groups were significantly different (R > 0.5); finally, July (P2) and August (P3) showed a well-separated community composition for abundance (R > 0.75). Biomass followed a similar statistical pattern to the community composition.

The result of SIMPER analysis is represented on Table 5. The highest average dissimilarities were found between July (P2) and August (P3) for abundance (δ = 54.45), and between May and June (P1) and July (P2) for biomass (δ = 66.01). May-June (P1) and August (P3) were the most similar periods for both abundance and biomass data, confirming the values obtained in the ANOSIM test and the MDS ordination. *Chaetoceros* spp., *Thalassiosira* spp., *Lauderia* spp., *Detonula* spp., and *Pseudo-nitzschia* spp. were the main taxa contributing to the dissimilarities between July (P2) and the other periods. Figure 13 shows the temporal distribution of the main taxa contributing to the abundance and biomass dissimilarities between the different periods.

TABLE 5. – Taxa contribution (%) to the average (a) abundance and (b) biomass Bray-Curtis dissimilarity (δ), between the three defined sampling periods (P1, P2 and P3). Data were square root transformed. Taxa were selected until ~50% of the cumulative dissimilarity was attained (for taxa codes see Table 3).

Taxa Code	P1 and P2 (%)	Taxa Code	P1 and P3 (%)	Taxa Code	P2 and P3
(a) Abundance					
	δ = 51.01		δ = 48.60		δ = 54.87
Cha	16.79	Lep	8.05	Cha	13.38
ThaS	7.34	Cha	6.00	ThaS	5.89
Ske	5.73	Rhi	5.85	Lep	5.84
PSN	5.03	Ske	5.45	Ske	5.62
Lau	3.62	PSN	5.03	PSN	4.70
Det	3.31	Cry	4.01	Rhi	4.52
DPb	3.15	DNs	3.37	Lau	3.77
Lep	3.08	GmGr	3.06	GmGr	3.19
GuiS	2.55	Gym	2.99	Cry	2.99
		ProC	2.98		
		DPb	2.94		
Cumulative δ %	50.61		49.73		49.92
(b) Biomass					
	δ = 66.01		δ = 58.98		δ = 62.60
Cha	9.27	Rhi	10.12	ThaS	7.73
ThaS	8.47	ProP	5.54	Rhi	7.60
Gui	5.35	Tin	4.42	Cha	7.50
Lau	5.35	DNb	3.78	Lau	5.73
Det	5.08	GuiF	3.72	Gui	5.44
ProP	4.28	Cha	3.54	Det	5.06
Cos	4.22	Cer	3.40	DNb	3.23
Tin	3.51	Oli	3.28	Cer	3.20
Cer	3.33	Cos	2.93	Cos	2.92
GuiF	2.59	DNs	2.89	ProP	2.82
		Lau	2.78		
		Gui	2.64		
		GmGr	2.60		
Cumulative δ %	51.44		51.64		51.23

TABLE 6. – Abundance (10^3 cell. l^{-1}) of potentially HAB organisms (Hallegraeff, 1995; Pitcher and Calder, 2000; Smayda, 2000) from May to September (2001) at Sagres station. See Table 3 for taxa codes.

Period	Date	Taxa Codes PSN	Ale	Cer	Din	Gon	Gym	ProC	Scr
P1	24-May	32.9	-	0.7	0.7	-	6.7	-	-
	31-May	-	-	0.7	-	-	-	-	-
	07-Jun	2.2	-	3.3	0.7	1.9	7.4	1.3	1.3
	26-Jun	45.0	-	1.7	1.0	-	26.7	14.3	1.7
	03-Jul	105.1	-	2.6	2.6	-	39.7	1.3	-
P2									
	11-Jul	76.7	-	-	-	-	6.5	-	-
	18-Jul	104.1	-	0.7	-	-	3.9	-	-
	24-Jul	128.9	-	-	-	-	-	-	-
	31-Jul	71.8	-	-	-	-	3.3	-	3.8
P3	06-Aug	7.8	-	3.6	1.3	-	21.7	1.2	3.3
	14-Aug	29.6	11.2	2.4	-	-	4.9	19.8	3.6
	20-Aug	4.0	0.7	0.7	0.3	-	1.3	1.5	0.3
	29-Aug	22.3	-	2.3	2.3	-	47.2	19.3	16.8
	03-Sep	209.4	-	1.9	1.3	-	1.3	23.3	8.4

- defines no occurrence

Potentially HAB organisms

Identification was mainly done down to genus level, so differentiation of harmful species within each taxa was not detected. Nevertheless, Table 6 presents the temporal distribution of algal taxa associated with harmful algal bloom (HAB) events identified during the survey at Sagres. *Pseudo-nitzschia* spp., a taxon that includes toxic species associated with amnesic shellfish poisoning (ASP; Bates *et al*., 1998), had the highest values for abundance in July (P2; 178±58 x10^3 cell. l^{-1}). Water discolorations, commonly called red tides, are produced by

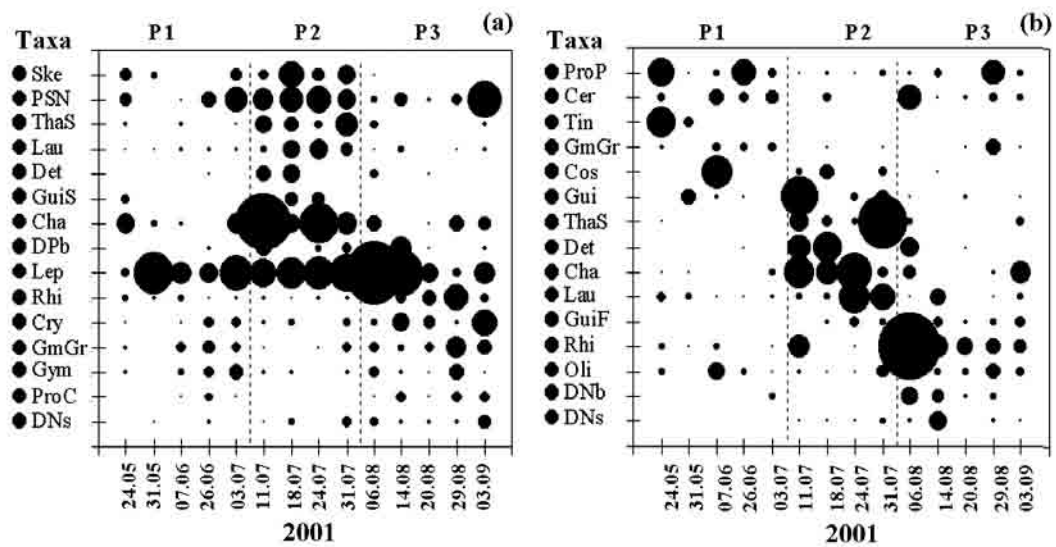

FIG. 13. – Temporal distribution of (a) abundance and (b) biomass of the main taxa contributing to Bray-Curtis dissimilarities between the defined sampling periods: P1, P2 and P3 (see Table 3 for taxa codes). Circles are proportional to abundance (max. 637 10^3 cell. l^{-1}) and biomass (max. 390 μgC l^{-1}) values; to avoid overlapping of circles, they represent 50% of their original size; as such, the absence of a bubble does not necessarily mean no occurrence, but that the relative abundance is low.

Ceratium spp., *Gonyaulax* spp., and *Scrippsiella* spp., amongst other organisms (Pitcher and Calder, 2000; Smayda, 2000). These blooms, although non-toxic, are undesirable because they may cause fish and invertebrate killings due to oxygen depletion, following the decay of the blooms. *Ceratium* spp. occurred at low values (< 4 x10^3 cell. l^{-1}) and was basically characteristic of May-June (P1) and August (P3). *Gonyaulax* spp. only occurred once in May-June (P1), and *Scrippsiella* spp. was prominent in August (P3; 0.3-16.8 x10^3 cell. l^{-1}). Organisms with the potential to cause paralytic shellfish poisoning (PSP), such as *Alexandrium* spp. and *Gymnodinium* spp., were also recorded. *Alexandrium* spp. occurred only in low numbers in August, whilst *Gymnodinium* spp. occurred throughout the survey, with the greatest abundance in May-June (P1) and August (P3; 47 x 10^3 cell l^{-1}). *Dinophysis* spp. and *Prorocentrum* spp., related to diarrhetic shellfish poisoning (DSP), were absent in July (P2), but occurred in May-June (P1) and August (P3).

DISCUSSION

Physical events and microplankton assemblage

Although the lack of sufficient vertical data limits an understanding of the whole dynamics in three-dimensions of the study site, the results show that during the upwelling season the Sagres region is influenced by the wind-driven circulation along the south and west coast, which forces cold, upwelled water into the surface layer. Upwelled water masses have characteristics of the ENACW subtropical branch (temperature > 13°C, σ_t < 27.1 kg m^{-3}). These findings are consistent with the patterns already described for the Algarve coast (Fiúza, 1983, 1984; Sousa and Bricaud, 1992). Winds are mostly moderate (6-8 m s^{-1}), and relatively intense velocities (8-10 m s^{-1}) are only registered in July (P2), revealing a decrease in wind stress conditions in comparison with previous years (Relvas and Barton, 2002). The influence of the warm counterflow on the south coast during episodes of relaxation (Relvas and Barton, 2002) has been noticed on several occasions.

Chl *a* peaks earlier (July) than has been reported (September) for the same area by Villa *et al.* (1997), probably owing to the interannual variability of physical factors (Peliz and Fiúza, 1999). The seasonal values for chl *a* and chemical parameters are in general agreement with the ranges described for the Cabo S. Vicente region (Moita, 2001). However, lower values of phosphate and silicate may imply the occurrence of a spring-bloom before the beginning of the survey. The maximal values for chl *a* (6.2 μg l^{-1}) attained in July are similar to those reported for the upwelling regions of NW Spain – La Coruña (6.7 μg l^{-1} Casas *et al.*, 1999) and Chile (6.2 μg l^{-1}, Daneri *et al.*, 2000), but lower than those of other upwelling systems such as Orgeon (1-57 μg l^{-1}, Dickson and Wheeler, 1995), Benguela, NW Africa, and off Peru (5-50 μg l^{-1}, Andrews and Hutchings, 1980; Estrada, 1974; Blasco, 1971 respectively). The lack of correlation between the Secchi-depth and chl *a* (Fig. 7), particularly during the bloom stage in July (P2) when Secchi values did not decrease as expected, may be due to several factors. The Secchi-disk depth is a measure of the concentration of light attenuating particles in the water column, whether from phytoplankton or non-phytoplankton sources. Factors contributing to the variation in Secchi-depth include the sun angle, sea surface reflectance and tidal height (Edmonson, 1980; Preisendorfer, 1986, Borkman and Smayda, 1998). In the current study, observations have been made independently of tidal phase. It may also be associated with variability in changes in chl *a* content per cell, carbon:chl *a* ratio, or chl *a* to accessory pigment ratio (Falkwoski and LaRoche, 1991).

Several upwelling pulses were registered from late spring to late summer (Fig. 3). The first pulse in June (P1) fertilises the surface water with nutrients, but its evolution was not followed by this survey. A more persistent-active upwelling event develops in July (P2), fertilising the surface with concentrations of nitrate up to 19 μM. This value is higher than that reported for NW Spain (La Coruña, 9.8 μM, Casas *et al.*, 1999; Ria de Vigo, 12 μM, Moncoiffé *et al.*, 2000).

Diatom biomass and density is dominant throughout the survey, and its temporal evolution is positively correlated (Spearman, $p<0.05$) with chl *a* and negatively correlated with SST, implying an association with cold waters supplied by upwelling. The maximal diatom abundance (1366 x10^3 cell. l^{-1}) is typical for other upwelling regions (10^6 cell. l^{-1}, refs. in Moita, 2001): NW Iberian-Galicia (Estrada, 1984), NW Africa (Blasco *et al.*, 1980), Peru (Blasco, 1971) and Benguela (Giraudeau *et al.*, 1993). The persistent diatom-chl *a* peak (≈ 21 days in July, P2) is related to prolonged conditions favourable to upwelling. This group is adapted to turbulent conditions (Margalef, 1978). The fact that

ammonium peaks are not coincident with oxygen minima, together with the predominance of low ammonium levels (< 0.5 µM), may imply pelagic nutrient regeneration as a secondary process during the survey period. Positively or neutrally buoyant diatoms could also partially explain the persistent bloom (refs. in Tremblay *et al*., 2002).

The bloom collapse seems to be associated with a decrease in conditions favourable to upwelling, together with episodes of stratification in the water column, probably caused by the influence of the warm countercurrent. Nevertheless, the transition to a well-established stratified surface layer, which is a condition for the development of the classical diatom-dinoflagellate succession (Margalef, 1978), does not occur because of the fortnightly cycles of upwelling and relaxation, typical of temperate upwelling conditions (Walsh *et al*., 1977).

Dinoflagellate abundance is positively correlated (Spearman, $p<0.05$) with temperature, suggesting an association with the warm waters of the countercurrent. *Lingulodinium polyedrum* has been described for this location by Amorim *et al*. (2004). Its absence from the samples in this study may be due to the sampling hour (early morning), when diel vertical migration limits its presence in surface waters, or to the inclusion of this species in higher classification groups. This species seems to be associated with coastal retention conditions in the Sagres area that may develop at times of relaxation when the cold waters are replaced by the warm waters of the countercurrent. Water retention has been reported in several upwelling areas (Graham and Largier, 1997; Demarcq and Faure, 2000; Marín *et al*., 2003). Coccolithophorids have been observed in the Cabo S. Vicente region (Abrantes and Moita, 1999; Cachão and Moita, 2000), but they have not been quantified because the calcareous plates may be damaged by preservation with acidic Lugol's solution.

Statistical analysis shows a distinct planktonic assemblage for the major upwelling-bloom stage (July, P2). *Chaetoceros* spp. (max. 567 $x10^3$ cell. l^{-1}), *Thalassiosira* spp. (max. 95 $x10^3$ cell. l^{-1}), *Pseudo-nitzschia* spp. (max. 129 $x10^3$ cell. l^{-1}), *Lauderia* spp. (max. 67 $x10^3$ cell. l^{-1}), and *Detonula* spp. (max. 53 $x10^3$ cell. l^{-1}) are the main taxa contributing to the dissimilarities between the July (P2) upwelling-blooming period and the other sampling periods (P1 and P3). This is in agreement with Moita (2001), who classifies these taxa as coastal upwelling indicators during spring and summer for the Portuguese coast.

Potentially HAB

The *Pseudo-nitzschia* spp. reached high abundances (171 $x10^3$ cell. l^{-1}) during this study. Nevertheless, this taxon includes toxic and non-toxic organisms. In order to evaluate the potential harmful effects of this species, a joint study of occurrence of organisms and detection of total biotoxin and biotoxin per cell must be undertaken. In Portugal, IPIMAR is the National Reference Laboratory for biotoxins. Potentially harmful dinoflagellate taxa (*Alexandrium* spp., *Ceratium* spp., *Dinophysis* spp., *Gonyaulax* spp., *Gymnodinium* spp., *Prorocentrum* spp., and *Scripsiella* spp.) were also recorded. Since 1994, *Gymonidinium catenatum* blooms have been registered east of Cabo S. Vicente, and their presence seemed to be dependent on upwelling nutrient enrichment (Moita *et al*., 1998). Regarding *Dinophysis* spp., concentrations of < 500 cell. l^{-1} were already reported as agents of human intoxication in Portugal, leading to the closure of bivalve harvest (Vale, 1999). During this survey, higher concentrations were attained (max. 2600 cell. l^{-1}). These values fall within ranges previously described for the Portuguese coast (Moita and Silva, 2000; Palma *et al*., 1998).

In a region such as Sagres where bivalve culture occurs, precautionary closure of the zone should be carried out for abundances of 200-1000 cell. l^{-1} for *Dinophysis* spp., *Gymnodinium catenatum,* and *Alexandrium minutum* and > 100000 cell. l^{-1} for *Pseudo-nitzschia* spp. (European Commission, 2002). The closure should be maintained until the respective biotoxin analysis is found to be negative.

Production and respiration rates

Production maxima are attained in July, concurrent with the diatom-chl *a* peak. The seasonal average of volumetric GP (25.4±19.8 µM O_2 d^{-1}) is higher than for the systems of Chile (11.5 µM O_2 d^{-1}; Daneri *et al*., 2000), Arabian Sea (6.8 µM O_2 d^{-1}; Robinson and Williams, 1999), NW Africa and Benguela (15.2 µM O_2 d^{-1}, 14.4 µM O_2 d^{-1} respectively, Robinson *et al*., 2002), but lower than for the Ría de Vigo-NW Spain area (37.3±30.7 µM O_2 d^{-1}, Moncoifée *et al*., 2000). DCR, on the other hand, is generally lower than reported for the above systems, representing only 17% of the GP, which reflects the predominance of the autotrophic component throughout the survey. The high significant correlations between total microplankton, chl

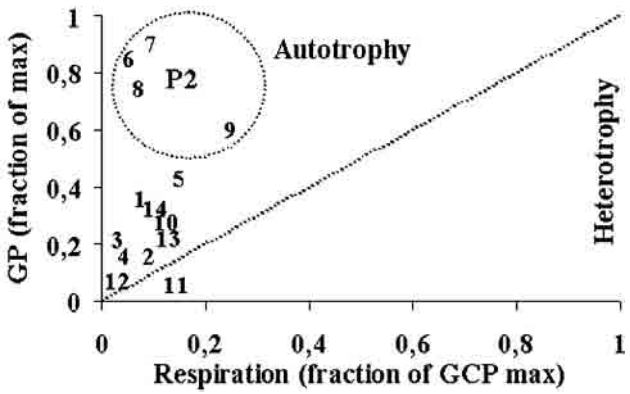

FIG. 14. – Phase plot of gross production (GP) versus respiration. Numbers indicate the temporal sequence of sampling dates (1= 24 May; 2= 31 May; 3= 7 June; 4= 26 June; 5= 3 July; 6= 11 July; 7= 18 July; 8= 24 July; 9= 31 July; 10= 6 August; 11= 14 August; 12= 20 August; 13= 29 August; 14= 3 September). P2 indicates the diatom-blooming period.

a, diatoms, production and oxygen data (Table 2) also suggest a dominant and active community of diatom-producers.

Following the approach of Blight *et al.* (1995), GP was plotted against respiration to study the phasing of these parameters (Fig. 14). It is generally observed that the autotrophic peaks are not coupled with heterotrophic maxima, denoting a temporal lag between the two processes. This feature has been reported for other coastal areas (e.g. Blight *et al.*, 1995; Robinson *et al.*, 1999) and is probably associated with natural physical loss mechanisms (dispersion, sedimentation) in upwelling areas. However, from date 4-5 (May-June, P1), and date 12-13 (August, P3), the increase in GP is related to an increase in respiration rates. Although the lack of bacterioplankton data limits the interpretation of these findings, high temperatures were recorded on day 5 and 13, which usually favours pico-heterotrophic activity (Wiebe *et al.*, 1993). Additionally, on both occasions there was a peak for ciliate abundance, the best biological predictor of DCR according to Spearman's correlation. A more efficient transfer from the auto- to the heterotrophic communities can be associated with a low molecular weight (LMW) pool of organic matter, originating from algal exudation, readily assimilated by heterotrophs (Blight *et al.*, 1995).

The autotrophic maximum (18 July) is coincident with the diatom bloom in July (P2). The heterotrophic maximum (31 July) is associated with a ciliate peak, together with a diatom maximum, a silicate minimum and a low PAR value, which suggests a co-limitation of light and nutrient on the diatom-photosynthetic rate (Kudela and Dugdale, 2000). The net heterotrophic period (NCP < 0) on 14 August occured during an episode in which nutrients were not limiting (nitrate: 8.5 μM; phosphate: 0.3 μM; silicate: 1.9 μM) but the value for PAR is low. This can be interpreted as a light limitation of the production rate (e.g. Ryther, 1956; Kirk, 1994). Cloud coverage can affect rates of production by a factor of up to 4.5 (Riegman and Colijn, 1991). Also, the decline in diatoms by this date is accompanied by an increase in the remaining functional groups (ciliate, dino- and nanoflagellate), contributing to a higher heterotrophic component. This transition period of the microplankton composition is probably associated with the intrusion of the warm coastal counterflow and the consequent stratification described above. As suggested for other systems (Moncoifée *et al.*, 2000; Robinson *et al.*, 2002), the observed heterotrophy could have been sustained by the accumulation of organic substrates from a recent bloom. The persistently high oxygen saturation (107%) measured at this time corroborates this hypothesis (Robinson *et al.*, 2002). A contribution to the dissolved organic matter pool from the excretion of hanging mussels has also been reported (Álvarez-Salgado *et al.*, 1996).

CONCLUSIONS

The Sagres area is subjected to the upwelling of cold waters in spring to late summer, originating in the wind-driven circulation patterns off the south and west coast. The temporal variation of these physical events regulates the influx of nutrients to the surface waters and subsequent microalgal growth, sustaining the phytoplankton biomass and production of the system. The long-lived diatom-chl *a* peak throughout July is probably associated with the persistence of the upwelling event. The collapse of this diatom bloom appears to be related to the decrease in upwelling conditions and the stratification of the water column, probably induced by the intrusion of the warm inshore water mass. These features imply a physical control of the biological development. *Chaetoceros* spp., *Thalassiosira* spp., *Lauderia* spp., *Detonula* spp., and *Pseudo-nitzschia* spp. can be considered as an upwelling proxy for this site. The progression of an upwelling / relaxation cycle determined the attained succession stage,

therefore regulating the composition of the microplankton assemblage and the subsequent nature of transfer to higher trophic levels, sediments and export. Low respiration rates (17% of GP) and uncoupling with production peaks appear to stem mainly from the interplay of the predominant autotrophic component and physical loss factors. Altogether, physical events seem to be the main factor influencing microplankton structure and production in this area.

More work needs to be done to understand the whole dynamic of this ecological productive system, including water-column studies of new production, bacterial rates, regeneration processes and grazing pressure. Also, the benthic and atmospheric domain awaits further study to improve the understanding of the ecosystem behaviour. Nevertheless, the present study brings a valuable insight into the productive waters of the Sagres area.

ACKNOWLEDGEMENTS

We are grateful to J.-M. Novalet (Sagremarisco, Portugal) and J. Llinas (UTM, Catalunya, Spain) for their technical support and help during sampling. We thank the team of the Delegação dos Portos do Sul, Sagres, for their assistance and supply of a working space, and N. Amado for help during sampling. We thank the NERC (Natural Environment Research Council) RSDAS (Remote Sensing Data Analysis Service), hosted by the PML (Plymouth Marine Laboratory), for providing the SST satellite images, and Dr Á. Peliz (IPIMAR, Portugal) for help with the satellite data. Thanks are also due to P. Puyana and H. Martins (Uni. Algarve, Portugal) for their assistance during nutrient and chl *a* analysis. We thank Prof. J. Ros (Univ. Barcelona, Catalonia, Spain), Dr D. Vaqué (ICM, Catalonia, Spain) and Prof. M. Castro (Univ. Algarve, Portugal) for their scientific and statistical advice, and appreciate the help of Prof. P. Relvas (Univ. Algarve, Portugal) in the graphic representation of wind data and scientific advice. This research was partially funded by FCT (Fundação para a Ciência e a Tecnologia, Portugal) project (PRAXIS-MAR 1696-95), and an FCT grant (Praxis XXI/BD/15840/98), within the III Quadro Comunitário de Apoio by FSE and MCES, funding S. Loureiro. We would like to express our gratitude to Dr T. Moita (IPIMAR, Portugal) for the review and valuable comments that improved this manuscript.

REFERENCES

Abrantes, F. and M.T. Moita. – 1999. Water column and recent sediments data on diatoms and coccolithophorids, off Portugal, confirm sediment record of upwelling events. *Oceanol. Acta*, 22(3): 319-336.

Álvarez-Salgado, X.A., G. Rosón, F.F. Pérez, F.G. Figueiras and Y. Pazos. – 1996. Nitrogen cycling in an estuarine upwelling system, the Ria de Arousa (NW Spain) I. Short-time-scale patterns of hydrodynamic and biogeochemical circulation. *Mar. Ecol. Prog. Ser.*, 135: 259-273.

Amorim, A.J. Moita and P. Oliveira. – 2004. Dinoflagellate blooms related to coastal upwelling plumes off Portugal. *Proc. of 10th Int. Conf. Harmful Algae*, Florida, USA. In press.

Andrews, W.R.H. and L. Hutchings. – 1980. Upwelling in the southern Benguela current. *Prog. Oceanogr.*, 9(1): 81 pp.

Bakun, A. – 1973. Coastal upwelling indices, west coast of North America, 1946-71. *NOAA Tech. Rep. NMFS SSRF-671. US Dept of Commerce, Seattle*: 103 pp.

Barber, R.T. and R.L. Smith. – 1981. Coastal upwelling ecosystems. *In:* Longhurst, AR (eds.): *Analysis of marine ecosystems*, pp. 31-68. Academic Press, New York.

Bates, S.S., D.L. Garrison and R.A. Horner. – 1998. Bloom dynamics and physiology of domoic-acid producing *Pseudo-nitzschia* species. *In:* Anderson, D.M. and A.D. Cembella (eds.): *Physiological Ecology of Harmful Algal Bloom*, pp. 267-292. NATO ASI Ser. 41, Springer, Berlin, Germany.

Bettencourt, A.M., S.B. Bricker, J.G. Ferreira, A. Franco, J.C. Marques, J.J. Melo, A. Nobre, L. Ramos, C.S. Reis, F. Salas, M.C. Silva, T. Simas and W.J. Wolff. – 2004. Typology and Reference Conditions for Portuguese Transitional and Coastal Waters. Development of Guidelines for the Application of the European Union Water Framework Directive. *INAG and IMAR, Lisbon, Portugal*: 96 pp.

Blasco, D. – 1971. Composition and distribution of phytoplankton in the region of upwelling off the coast of Peru. *Invest. Pesq.*, 35: 61-112.

Blasco, D., M. Estrada and B. Jones. – 1980. Relationship between the phytoplankton distribution and composition and the hydrography in the northwest African upwelling region near Cape Corbeiro. *Deep-Sea Res.*, Part A 27: 799-821.

Blight, S.P., T.L. Bentley, D. Lefèvre, C. Robinson, R. Rodrigues, J. Rowlands and P.J. leB Williams. – 1995. Phasing of autotrophic and heterotrophic plankton metabolism in a temperate coastal ecosystem. *Mar. Ecol. Prog. Ser.*, 128: 61-75.

Borkman, D.G. and T.J. Smayda. – 1998. Long-term trends in water clarity revealed by Secchi-disk measurements in lower Narragansett Bay. *ICES J. Mar. Sci.*, 55: 668-679.

Bryan, J.R., J.P. Riley and P.J. leB Williams. – 1976. A Winkler procedure for making precise measures of oxygen concentration for productivity and related studies. *J. Exp. Mar. Biol. Ecol.*, 21: 191-197.

Cachão, M. and M.T. Moita. – 2000. *Coccolithus pelagicus*, a productivity proxy related to moderate fronts off Western Iberia. *Mar. Micropaleontol.*, 39(1-4): 131-155.

Cachola, R. – 1995. Aquacultura «offshore» em Sagres. *8º Congresso do Algarve, Vilamoura, Portugal*: 861-867.

Casas, B., M. Varela, M. Canle, N. González and A. Bode. – 1997. Seasonal Variation of Nutrients, Seston and Phytoplankton, and Upwelling Intensity off La Coruña (NW Spain). *Est. Coast. Shelf Sci.*, 44: 767-778.

Casas, B., M. Varela and A. Bode. – 1999. Seasonal succession of phytoplankton species on the coast of A Coruña (Galicia, northwest Spain). *Bol. Inst. Esp. Oceanogr.*, 15(1-4): 413-429.

Clarke, K.R. and M. Ainsworth. – 1993. A method of linking multivariate community structure to environmental variables. *Mar. Ecol. Prog. Ser.*, 92: 205-219.

Clarke, K.R. and R.M. Warwick. – 2001. A further biodiversity index applicable to species lists: variation in taxonomic distinctness. *Mar. Ecol. Prog. Ser.*, 216: 265-278.

Daneri, G., V. Dellarossa, R. Quiñones, B. Jacob, P. Montero and O. Ulloa. – 2000. Primary production and community respiration in the Humboldt Current System off Chile and associated oceanic areas. *Mar. Ecol. Prog. Ser.*, 197: 41-49.

Demarcq, H. and V. Faure. – 2000. Coastal upwelling and associated retention indices derived from satellite SST. Application to *Octopus vulgaris* recruitment. *Oceanol. Acta*, 23(4): 391-408.

Dickson, M.L. and P.A. Wheeler. – 1995. Nitrate rates in coastal upwelling regime: a comparison on PN-specific, absolute, and Chl *a*-specific rates. *Limnol. Oceanogr*., 40(3): 533-543.
Edmonson, W.T. – 1980. Secchi disk and chlorophyll. *Limnol. Oceanog*r., 25: 378-379.
Estrada, M. – 1974. Photosynthetic pigments and productivity in the upwelling region of NW Africa. *Tethys*, 6: 247-260.
Estrada, M. – 1984. Phytoplankton distribution and composition off the coast of Galicia (northwest Spain). *J. Plankton Res*., 6: 417-434.
European Commission. – 1999. Report, Directive 91/494/EEC (Bivalve Molluscs) Portugal, Evaluation Mission (12-19.02.1999). *Directorate-General XXIV, Consumer Policy and Consumer Health Protection*, 8 pp.
European Commission. – 2002. Report of a mission carried out in Portugal from 21 January to 1 February 2001 regarding the implementation of Council Directive 91/493/EEC (fishery products), Council Directive 91/494/EEC (live bivalve molluscs). *Health and Consumer Protection Directorate-General*: 32 pp.
Falkwoski, P.G. and J. LaRoche. – 1991. Acclimation to spectral irradiance in algae. *J. Phycol*., 27: 8-14.
Fiúza, A.F.G., M.E. Macedo and M.R. Guerreiro. – 1982. Climatological space and time variation of the Portuguese coastal upwelling. *Oceanol. Acta*, 5(1): 31-40.
Fiúza, A.F.G. – 1983. Upwelling patterns off Portugal. *In:* Suess, E. and J. Thiede (eds.): *Coastal Upwelling: its sedimentary record. Part A. Responses of the Sedimentary Regime to Present Coast Upwelling*, pp. 85-98. New York: Plenum.
Fiúza, A.F.G. – 1984. *Hidrologia e Dinâmica das Águas Costeiras de Portugal*. PhD thesis, University of Lisbon, Portugal.
Fofonoff, N.P. and R.C.J.r. Millard. – 1983. Algorithms for computation of fundamental properties of seawater. *UNESCO Tech. Pap. Mar. Sci*., 44: 53 pp.
Graham, W.M. and J.L. Largier. – 1997. Upwelling shadows as near-shore retention sites: the example of northern Monterey Bay. *Cont. Shelf Res*., 17: 509-532.
Giraudeau, J., P.M.S. Monteiro and K. Nikodemus. – 1993. Distribution and malformation of living coccolithophores in the northern Benguela upwelling system off Namibia. *Mar. Micropaleontol*., 22(1-2): 93-110.
Grasshoff, K., M. Ehrhardt and K. Kremling. – 1983. *Methods of Seawater Analysis*. Verlag Chemie. FR Germany.
Hallegraeff, G.M. – 1995. Harmful algal blooms: a global overview. *In:* Hallegraeff, G.M. and D.M. Anderson (eds.): *Manual on Harmful Marine Microalgae*, pp. 1-22. IOC Man. Guides 33 Unesco, Paris, France.
Hillebrand, H., C.D. Dürselen, D. Kirschtel, U. Pollinger and T. Zohary. – 1999. Biovolume calculation for pelagic and benthic microalgae. *J. Phycol*., 35: 403-424.
JGOFS. – 1994. Protocols for the joint global ocean flux study (JGOFS) core measurements. *IOC Man. Guides*, 29: 170 pp.
Kirk, J.T.O. – 1994. *Light and Photosynthesis in Aquatic Ecosystems*, 2nd ed. Cambridge University Press, Cambridge.
Kudela, R.M. and R.C. Dugdale. – 2000. Nutrient regulation of phytoplankton productivity in Monterey Bay, California. *Deep-Sea Res*., Part II 47 : 1023-1053.
Large, W.G. and S. Pond. – 1982. Sensible and latent heat flux measurements over the oceans. *J. Phys. Oceanogr*., 12: 464-482.
Laws, E.A. – 1991. Photosynthetic quotients, new production and net community production in the open ocean. *Deep-Sea Res*., 38: 143-167.
Margalef, R. – 1978. Life-forms of phytoplankton as survival alternatives in an unstable environment. *Oceanol. Acta*, 1 (4): 493-509.
Marín, V.H., L.E. Delgado and R. Escribano. – 2003. Upwelling shadows at Mejillones Bay (northern Chilean coast): a remote sensing *in situ* analysis. *Inves. Mar*. 31(2): 47-55.
Martins, R. and M. Carneiro. – 1997. Contribuição para a caracterização da pesca artesanal local do Algarve. *9º Congresso do Algarve, Vilamoura, Portugal*: 437-442.
Moita, M.T., M.G. Vilarinho and A.S. Palma. – 1998. On the variability of *Gymnodinium catenatum* blooms in Portuguese waters. *In:* Reguera, B., B. Blanco and M.L. Fernández (eds.): *Harmful Algae*, pp. 118-121. Xunta de Galicia and IOC of UNESCO.
Moita, M.T. and A.J. Silva. – 2000. Dynamics of *Dinophysis acuta*, *D. acuminata*, *D. tripos* and *Gymnodinium catenatum* during an upwelling event off the Northwest Coast of Portugal. *In:* Hallegraeff, G.M., S.I. Blackburn and C.J. Bolch (eds.): *Harmful Algal Blooms 2000*, pp. 169-172. IOC of UNESCO.
Moita, M.T. – 2001. *Estrutura, Variabilidade e Dinâmica do Fitoplâncton na Costa de Portugal Continental*. PhD thesis, University of Lisbon, Portugal: 272 pp.
Moncoiffé, G., X.A. Álvarez-Salgado, F.G. Figueiras and G. Savidge. – 2000. Seasonal and short-time-scale dynamics of microplankton community production and respiration in an inshore upwelling system. *Mar. Ecol. Prog. Ser*., 196: 111-126.
Nykjăr, L. and L.V. Camp. – 1994. Seasonal and interannual variability of coastal upwelling along northwest Africa and Portugal from 1981 to 1991. *J. Geophys. Res*., 99 (C7): 14197-14207.
Officer, C.B. and J.H. Ryther. – 1980. The possible importance of Silicon in marine eutrophication. *Mar. Ecol. Prog. Ser*., 3: 83-91.
Palma, A.S., M.G. Vilarinho and M.T. Moita. – 1998. Interannual trends in the longshore variation of *Dinophysis* off the Portuguese Coast. *In:* Reguera, B., B. Blanco and M.L. Fernández (eds.): *Harmful Algae*, pp. 124-127. Xunta de Galicia and IOC of UNESCO.
Peliz, A.J. and A.F.G. Fiúza. – 1999. Temporal and spatial variability of CZCS-derived phtyoplankton pigment concentrations off the western Iberian Peninsula. *Int. J. Remote Sensing*, 20(7): 1363-1403.
Pita, C., A. Marques, K. Erzini, I. Noronha, D. Houlihan and M.T. Dinis. – 2002. Socio-economics of the Algarve (south of Portugal) fisheries sector. *Eur. Assoc. Fish. Eco. (EAFE) Conference, Uni. Algarve, Portugal*: 12 pp.
Pitcher, G.C. and D. Calder. – 2000. Harmful Algal Blooms of the Southern Benguela Current: a Review and Appraisal of Monitoring from 1989 to 1997. *S. Afr. J. Mar. Sci*., 22: 255-271.
Preisendorfer, R.W. – 1986. Secchi disk science: visual optics of natural waters. *Limnol. Oceanogr*., 31: 909-926.
Relvas, P. and E.D. Barton. – 2002. Mesoscale patterns in the Cape São Vicente (Iberian Peninsula). *J. Geophys. Res*.,107(C10): 28-1-28-23.
Riegman, R. and F. Colijn. – 1991. Evaluation of measurements and calculation of primary production in the Dogger Bank area (North Sea) in summer 1988. *Mar. Ecol. Prog. Ser*., 69: 125-132.
Robinson, C. and P.J. leB Williams. – 1999. Plankton net community production and dark respiration in the Arabian Sea during September 1994. *Deep-Sea Res*., Part II 46: 745-765.
Robinson, C., S.D. Archer and P.J. leB Williams. – 1999. Microbial dynamics in coastal waters of East Antarctica: plankton production and respiration. *Mar. Ecol. Prog. Ser*., 180: 23-36.
Robinson, C., P. Serret, G. Tilstone, E. Teira, M.V. Zubkov, A.P. Rees and E.M.S. Woodward. – 2002. Plankton respiration in the Eastern Atlantic Ocean. *Deep-Sea Res*., Part I 49: 787-813.
Ryther, J.H. – 1956. Photosynthesis in the Ocean as a Function of Light Intensity. *Limnol. Oceanogr*., 1(1): 61-70.
Ríos, A.F., F.F. Pérez and F. Fraga. – 1992. Water masses in the upper and middle North Atlantic Ocean east of the Azores. *Deep-Sea Res*., 39(3-4): 645-658.
Sampayo, M.A.M., S. Franca, I. Sousa, P. Alvito, P. Vale, M.J. Botelho, S. Rodrigues and A. Vieira. – 1997. Dez anos de monitorização de biotoxinas marinhas em Portugal (1986-1996). *Arq. Inst. Nac. Saúde*, 23: 187-194.
Smayda, T.J. – 2000. Ecological features of harmful algal blooms in coastal upwelling ecosystems. *S. Afr. J. Mar. Sci*., 22: 219-253.
Sousa, F.M. and A. Bricaud. – 1992. Satellite-Derived Phytoplankton Pigment Structures in the Portuguese Upwelling Area. *J. Geophys. Res*., 97(C7): 11343-11356.
Strickland, J.D.H. and T.R. Parsons. – 1972. A practical handbook of seawater analysis. 2nd ed. *Bull. Fish. Res. Board Can*., 167, 310 pp.
Tomas, C.R. – 1997. Identifying Marine Phytoplankton. *Academic Press, London*.
Tremblay, J.E., Y. Gratton, J. Fauchot and N.M. Price. – 2002. Climatic and oceanic forcing of new, net, and diatom production in the North Water. *Deep-Sea Res*., II 49: 4927-4946.
Utermöhl, H. – 1958. Zur Vervolkommnung der quantitativen Phytoplankton-Methodik. *Mitt. int. Verein theor. angew. Limnol*., 9: 1-38.
Vale, P. – 1999. *Caracterização de toxinas DSP na costa Portuguesa*. PhD thesis, University of Lisbon, Portugal.
Verity, P.G. and C. Langdon. – 1984. Relationships between lorica volume, carbon, nitrogen, and ATP contents of tintinnids in Narrangansett Bay. *J. Plankton Res*., 6: 859-868.
Verity, P.G., C.Y. Robertson, C.R. Tronzo, M.G. Andrews, J.R. Nelson and M.E. Sieracki. – 1992. Relationships between cell

volume and the carbon and nitrogen content of marine photosynthetic nanoplankton. *Limnol. Oceanogr.*, 37(7): 1434-1446.
Villa, H., J. Quintela, M.L. Coelho, J.D. Icely and J.P. Andrade. – 1997. Phytoplankton biomass and zooplankton abundance on the south of Portugal (Sagres), with special reference to spawning of *Loligo vulgaris*. *Sci. Mar.*, 61(2): 123-129.
Walsh, J.J., T.W. Whitledge, J.C. Kelley, S.A. Huntsman and B.D. Pillsbury. – 1977. Further transition states of the Baja California upwelling ecosystem. *Limnol. Oceanogr.*, 22: 264-280.
WFD - 2000. Directive 2000/60/EC of the European Parliament and of the Council. *Off. J. Eur. Comm.*, L 327: 1-73.
Wiebe, W.J., W.M. Sheldon and L.R. Pomeroy. – 1993. Evidence for an enhanced substrate requirement by marine mesophilic bacterial isolates at minimal growth temperatures. *Microb. Ecol.*, 25: 151-159.
Williams, P.J. leB. – 1981. Microbial contribution to overall marine plankton metabolism: direct measurements of respiration. *Oceanol. Acta*, 4(3): 359-363.
Williams, P.J. leB. – 1984. A review of measurements of respiration rates of marine plankton populations. *In:* Hobbie, J.E. and P.J. Williams, leB (eds.): *Heterotrophic activity in the sea*, pp. 357-389. Plenum Press, London.
Williams, P.J. leB. – 1998. The balance of plankton respiration and photosynthesis in the open oceans. *Nature*, 394: 55-57.
Wooster, W.S., A. Bakun and D.R. McLain. – 1976. The seasonal upwelling cycle along the eastern boundary of the North Atlantic. *J. Mar. Res.*, (34) 2: 130-141.

Scient. ed.: D. Vaqué